Journal of Civil and Environmental Engineering Vol. 55 (2025), No. 1, Special Issues, 76-99

University of Tabriz

Journal of Civil and Environmental Engineering

Optimizing Water Allocation in a Changing Climate Utilizing WEAP and SSP5.85 Scenarios- A Case Study: Keshan Chai basin

Farahnaz khoramabadi [a], Bahador Fatehi-Nobarian [b], Sina Fard Moradinia [c,d*]

[a] *Ph.D. Candidate in Climatology, University of Isfahan, Isfahan, Iran*

[b] *Assistant Prof. Department of Civil Engineering of Hydraulic Structures, Ara. C. Islamic Azad University, Jolfa, Iran*

[c] *Department of Civil Engineering, Ta.C., Islamic Azad University, Tabriz, Iran*

[d] *Robotic and Soft Technologies Research Center, Ta.C., Islamic Azad University, Tabriz, Iran*

Received: 01 March2025; Received in revised form: 28 July 2025; Accepted: 02 August 2025

ABSTRACT:

This study investigates the potential effects of the Isar Dam on the water resources of a specific basin, considering the growing concern of climate change. This research comprehensively assesses the impacts of climate change on the Keshan Chai basin by integrating advanced methods such as the WEAP model, the SSP5.85 scenario of the IPCC Sixth Assessment Report, and Landsat satellite imagery an analysis of historical data reveals significant fluctuations in water flow within the Ravasjan River, likely caused by repeated occurrences of floods and droughts. To address these variations and ensure a more stable water supply, the Isar Dam is projected to deliver regulated water for various purposes: 14 million cubic meters annually for drinking water, 35 million cubic meters annually for agriculture, and 4 million cubic meters annually for environmental needs. Climate change simulations project a 5% increase in annual precipitation for the forecast period (2025-2065) compared to the observation period (1990-2020), raising concerns about increased flooding in the region. The study also identifies three distinct climatic types based on monthly precipitation distribution. The minimum environmental flow requirement is estimated at 5.0 cubic meters per second monthly. Scenario-based water demand modeling shows that in Scenario 1, 92% of Ozghan's demand and 47% of the development networks are met in 70% of cases, with full satisfaction in 30%. Scenario 2 achieves 90% and 45% in 70% of cases, fully met in 25%. Scenario 3 meets 77% and 38% in 70% of cases, with 23% full satisfaction. Precipitation variability between 2011 and 2020 has created challenges for water management. Principal component analysis indicates 62.19% and 15.98% of precipitation variance are explained.

KEYWORDS:

Sustainable water management, Climate change, WEAP Model, ANOVA.

1. Introduction

Scientific evidence demonstrates that human activities have played a major role in warming the Earth and altering precipitation patterns, leading to increased occurrences of extreme weather events such as storms, floods, droughts, and heatwaves (Feng, 2021; Fu et al., 2007). The Intergovernmental Panel on Climate Change (IPCC), established in 1995, has reported a rise in global average temperature of approximately 0.6°C during the 20th century, with projections suggesting a further increase of 1 to 3.5°C in the current century if greenhouse gas emissions continue unchecked. These climatic shifts have introduced major challenges to the sustainable management of water resources. In response to these challenges, this research employs the WEAP (Water Evaluation and Planning) model to assess

Publisher: Vice Chancellery for Research & Technology, University of Tabriz
https://doi.org/10.22034/CEEJ.2025.66162.2420
Online ISSN: 2717-4077
* Orcid Cod Corresponding Author: 0000-0000-0000-3539-7311
Tel.: +09143142619
E-mail addresses: farahnaz.khoramabadi@yahoo.com (Farahnaz Khoramabadi), bfatehinobarian@iau.ac.ir (Bahador Fatehi-Nobarian), fardmoradinia@iau.ac.ir (Sina Fard Moradinia).

the impacts of climate change on the Keshan Chai basin. The model enables simulation of complex hydrological systems, evaluation of water infrastructure such as dams, assessment of sectoral water demands, and analysis of flood risks. By applying the SSP5.85 scenario from the IPCC Sixth Assessment Report which reflects a future with high emissions and rapid economic growth this study examines a worst-case climate trajectory. Furthermore, the integration of high-resolution Landsat satellite imagery enhances the precision of water resource monitoring and model calibration. While previous studies have often relied on localized or single-model approaches, this research hypothesizes that combining advanced climate scenarios, satellite data, and the WEAP model can offer a more accurate and comprehensive understanding of quantitative and qualitative changes in water resources, thereby supporting more effective climate adaptation policies.

Malmir et al. (2018) investigated the impact of climate change on agricultural water allocation in the Qarasu watershed using the WEAP model. Their findings indicate that under future climate scenarios, with the current cultivated area remaining unchanged, agricultural water demand in the study area will increase. Moradian et al. (2019) conducted a multi-criteria evaluation of water allocation scenarios in water-scarce basins using the TOPSIS method and the WEAP model. The results showed that in the fully cooperative scenario, with water allocation to stakeholders and the use of the Shapley value method, the benefits of all stakeholders increase. This scenario can be proposed as an alternative to the water transfer scenario to this basin. In another study, Agha karami et al. (2012) utilized the WEAP model to conduct a quantitative assessment of different water allocation scenarios in the Tehran-Karaj plain. The aim of this study was to investigate the impacts of implementing a wastewater treatment and water transfer scheme from neighboring basins to Tehran on the groundwater and surface water resources of the Tehran-Karaj plain. Wang et al. (2019) investigated integrated water resource management and modeling in the Bo River Basin, Canada. Their study highlights that increasing the use of cooling towers in thermal power plants is the most effective strategy for managing water demand in the industrial sector. Sabbaghi et al. (2020) conducted a separate study examining the economic impacts of climate change on water resources and agriculture in the Zayandeh Rud Basin, Iran. Their findings indicate that by mid-century, precipitation in the Zayandeh Rud Basin will decrease significantly while temperatures will rise. Martinsen et al. (2019) addressed the joint optimization of water allocation and water quality management in the Haihe River Basin. They employed a linear optimization model to tackle this complex issue. This multi-reservoir, multi-period, and multi-objective model incorporated water quality considerations at various locations within the basin. Feng et al. (2021) explored optimal regional water resource allocation using a dynamic multi-objective balancing strategy. Water resource allocation faces several challenges, including uncertainty in water supply due to climate change, overlooking the dynamic allocation of water resources, and inappropriate allocation that can lead to tensions among water-consuming sectors. To address these challenges, an optimal water resource allocation model was developed using dynamic multi-objective programming and considering uncertainty in water supply. Yaghoubi et al. (2020) proposed an optimization model to develop operational rules for water reservoirs, considering water quality and climate change. The model was used to simulate various future climate and water demand scenarios. The results of this research, which will be carried out considering the various dimensions of this challenge, including temperature changes, precipitation, water distribution patterns and associated risks, can be the basis for adopting systematic policies and strategic planning in various sectors, including agriculture, water resource management, industry, etc. Dlamini et al. (2023) assessed the impact of climate change on surface water availability (SWA) in the Buffalo River watershed. It showed that climate change will increase rainfall, but also lead to more evapotranspiration and water demand. While SWA will increase slightly, it will not be enough to meet the growing demand. This study shows that the water-energy-food nexus approach can contribute to the development of sustainable water management strategies. Mejía et al. (2023) investigated current conditions and future changes in short-term events, low river discharge, and associated uncertainties in the San Pedro catchment. Peng et al. (2024) evaluated water resource safety in Guiyang from 2013 to 2022 using the DPESFR model and combined weighting methods. The results showed a declining trend in water resource safety. Key limiting factors were identified in the "status," "response," and "drive" subsystems. Predictions indicate a continued decline in water resource safety in the future. Kng et al. (2023) assessed changes in bivariate flood risks (peak and duration) and their socioeconomic impacts in 204 Chinese catchments using climate and hydrological models. Results project a significant increase in extreme flood risks in China, even under low emission scenarios, with substantial increases in the exposure of population and regional gross domestic product. Snizhko et al. (2024) used the WaterGAP2 hydrological model and SSP1-2.6 and SSP5-8.5 scenarios to assess changes in the flow of the Southern Bug River in Mykolaiv, Ukraine, under climate change. Results show that under the SSP1-2.6 scenario, the impact of climate change on river flow is insignificant,

while under the SSP5-8.5 scenario, a significant decrease in river flow is projected from May to October.

Daily precipitation and temperature projections from 19 advanced global climate models (CMIP6) and four future scenarios (SSP1-2.6, SSP2-4.5, SSP3-7.0, and SSP5-8.5) were reduced by adjusting the delta and using a more advanced quantile. Among these, three CMIP6 models were selected MIROC6, CanESM5, and IPSL-CM6A-LR based on their suitability for the region under study, considering past performance in representing historical precipitation and temperature trends. The selection was guided by regional relevance and alignment with literature that emphasizes the importance of model accuracy in localized climate impact studies. For example, while models such as MIROC-ES2L and IITM-ESM have shown strong performance in certain regions, their application in this study's geographical and climatic context was deemed less optimal due to discrepancies in precipitation simulations noted in regional evaluations. To further justify the selection, variance analysis was conducted to assess the uncertainty contribution of climate models, hydrological models, and extreme value distributions (EVDs) in the results. This approach ensures that the selected models are robust for simulating future climatic scenarios. Future work will explore ensemble approaches, as recommended in "Identification of Best CMIP6 Global Climate Model for Rainfall by Ensemble Implementation of MCDM Methods and Statistical Inference" and "Accuracy of historical precipitation from CMIP6 global climate models under diversified climatic features over India". These recommendations will be integrated to enhance the model selection process in subsequent studies. The study concludes that the Dhidhessa river basin is vulnerable to climate change and requires careful management to ensure water security. Chawanda et al. (2024) investigated the impact of climate change and land use land cover change (LULCC) on water resources in Africa. The study found that the Zambezi and Congo river basins are likely to experience reduced river flows due to climate change. While the Limpopo River is likely to have more river flow. The Niger River Basin is likely to experience the greatest decline in river flow. The Congo River Basin is particularly sensitive to LULCC and has a significant impact on river flow. These changes have implications for agriculture, energy and livelihoods in Africa. This research highlights the need to address climate change and deforestation to reduce the impact on water resources.

Ciampittiello et al. (2024) reviewed 320 articles on climate change and water resources. This research showed that climate change affects water resources by decreasing rainfall, increasing temperature and increasing water consumption by humans. The study suggests integrated water resources management, political action, increased knowledge and new technologies as solutions. It also emphasizes the importance of protecting and restoring ecosystems. The Italian political situation and potential measures for water resource management are also discussed. Zhou et al. (2024) have conducted a comprehensive study to assess the impact of climate change on hydropower generation. They employed a three-step framework involving hydrological and climate models to predict future reservoir inflows under various climate scenarios. By analyzing the uncertainties arising from different model structures, climate emission scenarios, and their interactions, they quantified the impact of these factors on hydropower generation at various time scales. The findings highlight the significant influence of these uncertainties, particularly during flood and non-flood seasons, and underscore the need for proactive measures to mitigate the negative consequences of climate change on hydropower energy development. Garnier et al. (2024) aimed to assess recent climate changes in the Chilean Altiplano by studying the fluctuations in water levels of three endorheic lakes: Chungará, Miscanti, and Miniques. They utilized a novel approach, leveraging the Google Earth Engine platform to analyze satellite imagery data from Landsat and MODIS. By extracting the shapes and calculating the surface areas of these lakes over a 31-year period, they were able to correlate these changes with precipitation data from meteorological stations and TRMM. The results consistently indicate a decline in both lake area and rainfall volume, suggesting a drying trend in the region. This study provides valuable insights into the impact of climate change on water resources in the Chilean Altiplano and highlights the potential of remote sensing techniques for monitoring hydrological changes in remote and data-scarce regions. Bañares et al. (2024) aimed to assess the impact of climate change and urbanization on water resources in the Philippines. They utilized the Water Evaluation and Planning (WEAP) software and climate forecasts from multiple Global Circulation Models (GCMs) to model the water balance in two sensitive watersheds: Libmanan-Pulantuna and Quinali. By creating various climate-urbanization scenarios, the study projected future water availability in these regions. This research provides valuable insights into the hydrological processes in these traditionally under-observed areas, contributing to future environmental planning and sustainable water management strategies in the Philippines and other similar regions. Hamlat et al. (2024) investigated the impact of climate change, policy options, technological development, and human behavior on water availability and demand in El Bayadh province, Algeria. They utilized the Water

Evaluation and Planning System (WEAP) model to assess multiple future scenarios and identified a significant water supply-demand gap, particularly impacting agricultural areas. The study highlights the need for long-term strategies to address water scarcity and proposes adaptive solutions to help water managers cope with complex water challenges in this arid region. Climate change and its associated impacts on precipitation and temperature patterns have been widely studied in recent years, with particular focus on understanding long-term trends and extreme weather events. Previous studies have extensively analyzed rainfall and temperature trends to identify the implications of climate variability and climate change on water resources, agriculture, and ecosystems.

For instance, Karmakar et al. (2021), in their study "Determine the best method for analysing long-term (120 years) annual and seasonal rainfall trends in four east India river basins," evaluated the performance of various statistical methods for detecting rainfall trends in the context of long-term climate variability. The authors demonstrated that Mann-Kendall and Sen's slope estimator provide robust results in identifying both annual and seasonal rainfall trends, highlighting the significance of method selection in climate change studies. Furthermore, studies have also focused on temperature extremes and their evolving trends over the decades.

Singh and Kumar (2022), in their research "Is the extreme temperature trend changed in the last two decades compared to the last seven decades?" provided insights into the intensification of extreme temperature events in recent decades. Their findings underscore a pronounced increase in the frequency and intensity of extreme temperature events in the past 20 years, indicating a shift in the baseline climate conditions due to anthropogenic influences. This study is particularly relevant for understanding the broader implications of changing temperature extremes on human health, energy demand, and agricultural productivity. In light of these findings, the current study builds upon these established methodologies and insights to analyze climate change impacts on the Keshan Chai Basin. By integrating both long-term trend analysis and extreme value assessment, this research aims to provide a comprehensive understanding of the ongoing changes in precipitation and temperature patterns under future climate scenarios. In this research, a comprehensive and multi-faceted approach was employed to investigate the interactive effects of climate change and dam construction on the water resources of the Keshan Chai Basin. Researchers combined hydrological modeling (using the WEAP model) with advanced statistical analyses to accurately simulate and assess the complex changes in climate and their impacts on the basin's water resources. To account for differences in the spatial and temporal resolution of the selected CMIP6 models (MIROC6, CanESM5, and IPSL-CM6A-LR), the climate data were downscaled to ensure consistency and comparability. Bias correction and statistical downscaling techniques were applied to adjust model outputs to a uniform resolution compatible with the study area's scale. These processes ensured that the discrepancies in resolution across models did not introduce bias into the hydrological simulations or the derived insights. Additionally, the NDWI index was utilized to monitor changes in soil moisture and vegetation as indicators of the basin's water status. By analyzing rainfall anomalies and their probability distributions, patterns of rainfall changes and the occurrence of droughts and floods in the region were identified. Furthermore, principal component analysis (PCA) was used to extract key features and identify hidden patterns in rainfall data. To enhance the credibility of the results, the developed models were compared and validated against data from the IPCC Sixth Assessment Report. Statistical methods such as ANOVA and linear regression were also employed to evaluate differences and relationships between various variables. Two databases were utilized to model the water resources of the Keshan Chai River catchment using the WEAP model.

The first database comprised comprehensive and detailed information regarding the physiographic, hydrologic, and land use characteristics of the catchment area. These data served as input for the WEAP model. Within the model, the various components of the basin, including rivers, reservoirs, and water demand, are schematically represented, and the relationships between them are defined. The second database contained climate data for the SSP5-8.5 scenario retrieved from the Sixth Climate Change Assessment Report (CMIP6). This data was freely available through the Global Climate Model Database (https://esgf-node.llnl.gov/search/cmip6). Following the calibration and validation of the WEAP model, various scenarios were implemented to simulate the development of water resources with the inclusion of the Isar Dam and the effects of climate change. These scenarios investigated the impact of dam construction on reservoir storage volume, river flow, and the provision of water needs for different sectors (agriculture, industry, drinking). This research introduces a novel approach to comprehensively assess the impacts of climate change on the Keshan Chai basin by integrating multiple advanced methods and tools. The Water Evaluation and Planning System (WEAP) model is employed as a robust tool for simulating water resource allocation, enabling the evaluation of both water quantity and quality under changing climatic conditions. The model's ability to simulate complex

hydrological systems and optimize water resource management makes it particularly suitable for this study. By utilizing the IPCC's Sixth Assessment Report and specifically focusing on the SSP5.85 scenario, which represents a high greenhouse gas emissions and rapid economic growth pathway, the research allows for an examination of a worst-case climate change scenario. This approach is crucial for water resources planning and management, as it provides valuable insights into potential risks and the need for adaptive strategies. Furthermore, the integration of Landsat satellite imagery offers a high spatial and temporal resolution for monitoring and analyzing the basin's water status. This innovative technique facilitates continuous and accurate assessment of changes in water levels and quality under the influence of climate change, providing up-to-date and reliable data for calibrating and validating the WEAP model. Based on previous studies that used less comprehensive model comparisons, the hypothesis of this research is that integrating the WEAP model with advanced climate scenarios and high-resolution satellite data will produce more accurate and holistic predictions of climate change impacts on water resources than single-model approaches. In summary, the novelty of this research lies in the combination of these tools and data to achieve a precise assessment and prediction of the impacts of climate change on water resources. The study offers data-driven and effective management strategies to address the challenges posed by a changing climate.

2. Materials and Methods

The Isar Dam is located in the Horand section of Ahar County, East Azerbaijan Province, Iran, on the Ravasjan River. The project's objectives are to expand the river's surface water resources and establish irrigation networks to supply the region with agricultural and drinking water. The study area encompasses the Kashafchai River Basin in northeastern Ahar, with a maximum elevation of 2814 meters above sea level at the Qabakh Tepeh heights and a minimum elevation of 1447 meters at the Rvasjan hydrometry station. The Keshan chai watershed is bordered by the Kalibar chai watershed to the north, the Ahar River to the south, the Baramis watershed to the west, and the channels leading to the Ahar River to the east. The general location of the project and the study area are shown in Fig. 1.

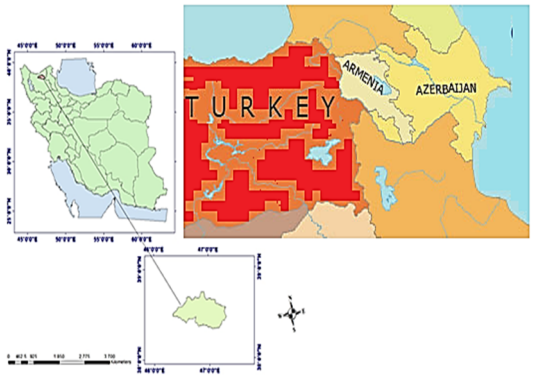

Fig. 1. General Location of the Project and Surrounding Areas (Technical Studies of Isar Dam, Ahar-Iran)

The data utilized in this research encompassed a wide range of climatic, physiographic, hydrological, and operational information, all of which were gathered from credible and diverse sources. Meteorological data (including precipitation, temperature, and evaporation) and river discharge records were collected from selected stations of the Iran Meteorological Organization and the East Azerbaijan Regional Water Company for the period 1990 to 2020. To ensure temporal continuity and data quality, the time series were thoroughly examined. In cases where gaps were identified, missing data were completed using linear interpolation and correlation with nearby stations. Physiographic data were obtained using maps, previous studies, and ArcGIS software. Future climate data were extracted from CMIP6 model outputs under the SSP5-8.5 scenario. Water demand data were derived from current consumption statistics and regional development plans.

GIS data were acquired from satellite imagery and spatial analysis tools, while operational data related to the dam were gathered through the Regional Water Company and processed using WEAP software. Furthermore, statistical analyses, including PCA and ANOVA, were conducted using XLStat, Minitab, and Excel. All data were completed, quality-checked, and pre-processed prior to being used in the modeling and final analysis phases.

In this research, necessary data were initially collected. To identify and analyze changes in surface water extent, the JRC Global Surface Water Mapping Layers (version 1.4) were utilized. These layers provide comprehensive information on the spatial distribution and temporal variations of surface water bodies. Subsequently, satellite imagery was employed to calculate the Normalized Difference Water Index (NDWI). This index effectively distinguishes water bodies from other surface covers. Moreover, data pertaining to the geometric characteristics of dams, including

height, reservoir volume, and surface water area, were gathered and integrated into the WEAP software for simulation purposes.

Rainfall data was extracted from the SSP5-8.5 scenario, a high socioeconomic pathway of greenhouse gas emissions, and associated climate models to forecast the potential impacts of climate change on rainfall patterns and water resources. Furthermore, historical and projected rainfall data obtained from climate models were analyzed to investigate the relationship between rainfall variations and changes in water area. In the phase dedicated to analyzing surface water changes, the NDWI was instrumental in differentiating surface water from other land covers. This index was computed using infrared and green bands from satellite imagery. Spatial and temporal variations in surface water extent were subsequently analyzed using the JRC Global Surface Water Mapping Layers dataset. To predict future rainfall patterns and examine their relationship with water changes, climate models and the SSP5-8.5 scenario were utilized. Rainfall projections were generated for future periods, and the relationship between rainfall and surface water variations was analyzed using Principal Component Analysis (PCA) and Analysis of Variance (ANOVA). Subsequently, the predicted rainfall data was incorporated into the WEAP model. In the section dedicated to water resources simulation and modeling, the WEAP software was employed to simulate the regional water resources system. This software facilitates the modeling of water flow, water resources management, and the evaluation of various management scenarios. In this simulation, the geometric characteristics of dams, such as height and reservoir volume, were incorporated to analyze their influence on water resources management. Furthermore, the SSP5-8.5 scenario and associated climate models were applied to predict the impact of climate change on water resources within the WEAP model. Finally, the results obtained from the analysis of surface water area changes, rainfall predictions, and WEAP simulations were compared and analyzed. In this research, xlstat, Excel, Minitab, ArcGIS, and WEAP software were utilized for data analysis and modeling. The research steps have been clearly presented in Table 1.

JRC Global Surface Water Mapping Layers, v1.4. This dataset, developed by the Joint Research Centre (JRC) of the European Commission, served as a comprehensive resource for analyzing the changes in water levels of Lake Urmia. Leveraging satellite data, these layers provide global-scale mapping of surface water distribution and dynamics, as detailed in Tables 2 and 3 (Jin et al., 2023).

SSP245, SSP370, Table 4 summarizes the specifications of the climate models and the SSP scenarios employed in this study. While the study initially focused on the SSP5-8.5 scenario, a high-emissions pathway, additional analyses were conducted to compare the effects of SSP2-4.5 (a medium stabilization scenario) and SSP3-7.0 (a medium-high emission scenario). These comparisons are critical for understanding the potential range of climate impacts under varying socioeconomic and emissions trajectories. The inclusion of SSP2-4.5 and SSP3-7.0 allows for a more comprehensive assessment of the uncertainties and variabilities associated with future projections. For SSP2-4.5, moderate mitigation efforts result in lower radiative forcing by 2100 compared to SSP5-8.5, leading to less severe climate impacts. SSP3-7.0, on the other hand, reflects a fragmented world with regional rivalries and slower mitigation efforts, resulting in intermediate radiative forcing levels.

These additional scenarios provide valuable insights into how the Keshan Chai Basin's water resources might respond under different future pathways. By incorporating multiple scenarios, the study better captures the range of possible outcomes and enhances its utility for regional planning and decision-making.

The incorporation of multiple SSP scenarios ensures that the study provides a robust and nuanced understanding of the potential impacts of climate change, offering insights that are more aligned with real-world decision-making requirements.

Table 1. Research Steps

1. Data Collection					
Meteorological Data (Precipitation, Temperature, Evaporation)	Hydrological Data (Streamflow/Discharge)	Physiographic Data (DEM, Land Use, Soil Maps)	Operational Data (Reservoir operations, Demand sectors)	Future Climate Scenarios (CMIP6-SSP5-8.5)	Water Demand Data (Current usage, Development plans)
2. Data Pre-processing					
Quality control and gap filling (Interpolation, correlation with nearby stations)	Spatial processing using GIS (ArcGIS)			Statistical analysis (PCA, ANOVA-XLStat, Minitab, Excel)	
3. Model Setup in WEAP					
→ Inputs: - Climatic Data - Streamflow Data - Demand Nodes - Reservoir Characteristics	→ Parameters: - Catchment runoff coefficients - Reservoir capacity curves (A-V-H)	→ Scenarios: - Baseline (Historical, 1990–2020) - Future (SSP5-8.5, 2020–2050)			
4. Model Simulation (Using WEAP)					
Water allocation simulation under climate change	Supply-Demand balance	Reservoir performance			
5. Output Analysis					
Streamflow variations	Deficit analysis in supply	Spatial and temporal changes in water availability	Scenario comparison		
6. Results and Conclusions					
Key findings with numerical outputs	Implications for water resources planning				

Table 2. Landsat time series and GEE datasets (Jin et al. 2023)

Landsat Time Series		Years	Datasets Data	Resolution
Years	Satellite Sensor			
		1984-2021	JRC Globat Surface Water Mapping Layers, v1.4 NASA SRTM DEM GLCF: Landsat Global Inland Water SinoLC-1	30m
`1990-1995	Landsat5TM	2000		
2000-2010	Landsat7 ETM+	2000		
2015-2022	Landsat8 OLI	2021		1m

Table 3. Definition and range of changes of JRC satellite bands for monitoring water level changes (https://earthengine.google.com/)

Bands					
Row	Name	Units	Min	Max	Description
4	Seasonality		0	12	Number of months water is present
6	Transition	---	0	10	Categorical classification of change between first and last year

Table 4. Characteristics of CMIP6 Climate Models (https://esgf-node.llnl.gov/status)

Model Name	Modeling nstitution	Spatial Resolution	Emission Scenario
CanESM5	Commonwealth Scientific and Industrial Research Organization (CSIR), Canadian	2.8×2.8m (Canada)	SSP2-4.5, SSP3-7.0, SSP5-8.5
CNRM-CM6	Centre National de Recherches Météorologiques- Climate Model version 6 (CNRM and Cerfacs)	0.5×0.5m (France)	SSP2-4.5, SSP3-7.0, SSP5-8.5
CMCC-ESM2	Centro Euro-Mediterraneo sui Cambiamenti Climatici-Earth System Model Version 2	1×1m (Italy)	SSP2-4.5, SSP3-7.0, SSP5-8.5

2.1. Model selection criteria

CNRM-CM6 Model: This model is used to simulate the Earth's past, present, and future climate (Figure 2). It is applied to study a wide range of climate phenomena, including climate change, global warming, extreme weather events, and climate cycles (Oki & Sud, 1998; Voldoire et al., 2019).

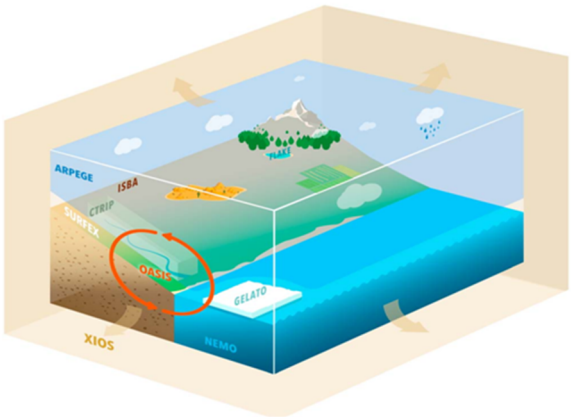

Fig. 2. Components of the CNRM-CM6-1 model, Source: (Voldoire et al., 2019)

CMCC-ESM2 Model: This model is capable of simulating historical climate change and predicting future climate under different greenhouse gas emission scenarios. This information is essential for understanding how climate is changing and its impacts on Earth systems (Lovato et al., 2022).
CanESM5 Model: This model excels in simulating one of the essential climate features: precipitation. It is employed to forecast century-scale climate patterns as well as generate seasonal and decadal predictions. As a forecasting tool, CanESM5 aids in developing optimal strategies for water resource management and decision-making related to watersheds (Swart et al., 2019: 4855; Khoramabadi & Fard Moradinia, 2024).

The choice of the SSP5-8.5 scenario aligns with the model selection criteria discussed earlier. The CNRM-CM6 model's ability to simulate extreme weather events under various climate conditions makes it suitable for exploring the severe precipitation changes projected under SSP5-8.5. Additionally, the CMCC-ESM2 model's capability in predicting future climate under different emission scenarios complements the analysis by providing insights into the potential range of precipitation changes under alternative scenarios. This combination of model capabilities and scenario selection enables a comprehensive assessment of the study area's vulnerability to climate change impacts.

2.2. WEAP (Water evaluation and planning system)

WEAP, developed by the Stockholm Environment Institute (SEI) in 1990, has emerged as a powerful tool for comprehensive watershed management and water resource planning (Li et al., 2015). By integrating and simulating various components of a watershed, WEAP empowers users to effectively manage and plan water resources. A key advantage of WEAP lies in its ability to simulate diverse development scenarios within a watershed. Utilizing WEAP, one can examine and simulate the impacts of factors such as population growth, changes in reservoir operation policies, groundwater withdrawals, artificial recharge schemes, water conservation measures, water allocation for ecosystem needs, conjunctive use of surface and groundwater, wastewater reuse, high-efficiency irrigation practices, changes in cropping patterns, climate change, pollutant effects, and land use changes on water resources (RaziSadath et al., 2023). In the hydrological modeling component, WEAP simulates all necessary processes for quantifying surface water balance and the interaction of groundwater aquifers with river flow (Huang, 2023).

2.3. Required data

Data can be provided in one of three formats: monthly time series, monthly averages, or constant parameters. The required data are listed in Table 5.

2.4. Streamflow

Statistical Period Used for Streamflow Estimation: 10-Year Period (2011-2021) Estimated Average Annual Streamflow at the Proposed Site of Isar Dam Reservoir: 9.2 Cubic Meters per Second (m^3/s).

2.5. Geometric characteristics of the dam

The geometric characteristics of the reservoir at the proposed axis have been prepared using a combination of 1:2000 and 1:10000 scale topographic maps. These characteristics include the elevation-area curve and the elevation-volume curve of the lake at different elevations. In the considered option, the riverbed elevation is 152 meters, and the lake area and volume at an elevation of 200 meters are 188.31 hectares and 29.05 million cubic meters, respectively. The elevation-area and elevation-volume curves are estimated in the WEAP model using two components: elevation and volume, and the cylinder equation for surface area. Figure 3 shows the variation of reservoir volume with respect to elevation.

Table 5. Required Data for Water Resource Planning Modeling of the Study Area

		Sub group 2	Sub group 3	Data Type
Resources and Uses	Sub group 1	Climate Data	Discharge Temperature Evaporation Wind Speed Latitude	Monthly Time Series Monthly Time Series Monthly Time Series Monthly Average Monthly Average
Demand Sites	Sub basin Nodes	Allocation Priority		Parameter
	Agricultural Demand Site	Water Use	Agricultural Land Area Annual Water Use Rate Consumption Rate	Parameter Parameter Parameter
Resources	River	Allocation Priority		Parameter
		Reservoir		Parameter
			Storage Volume Inactive Volume	Parameter Parameter
	Hydrometric station		Streamflow Data Percentage of Return Flow from Each Site to Each Source	DataTime Series Parameter

2.4. Streamflow

Statistical Period Used for Streamflow Estimation: 10-Year Period (2011-2021) Estimated Average Annual Streamflow at the Proposed Site of Isar Dam Reservoir: 9.2 Cubic Meters per Second (m^3/s).

2.5. Geometric characteristics of the dam

The geometric characteristics of the reservoir at the proposed axis have been prepared using a combination of 1:2000 and 1:10000 scale topographic maps. These characteristics include the elevation-area curve and the elevation-volume curve of the lake at different elevations. In the considered option, the riverbed elevation is 152 meters, and the lake area and volume at an elevation of 200 meters are 188.31 hectares and 29.05 million cubic meters, respectively. The elevation-area and elevation-volume curves are estimated in the WEAP model using two components: elevation and volume, and the cylinder equation for surface area. Figure 3 shows the variation of reservoir volume with respect to elevation.

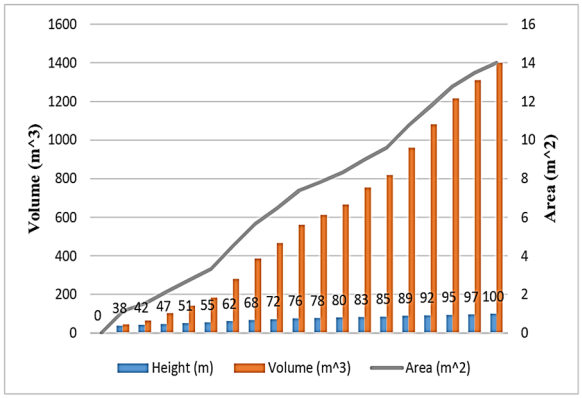

Fig. 3. A-V-H (Area-Volume-High) diagram

2.6. Evaporation

The evaporation rate from the free water surface at the proposed site has been estimated in the first phase of the meteorological studies of the design plan and will be used in the calculations. As shown in Fig. 4, and table 6 the annual evaporation from the free water surface is 1739.4 millimeters. In these studies, the direct rainfall volume on the lake surface has been neglected as a safety factor in the water supply potential of the reservoir.

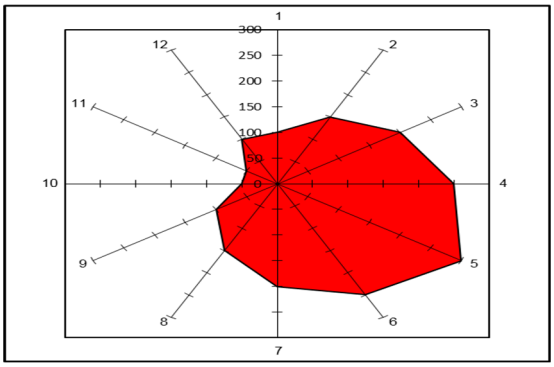

Fig. 4. Monthly Evaporation Values at Isar Dam Site

Table 6. Monthly Evaporation Values (mm)

Month	EV (mm)
October	149.054
November	101.872
December	56.1238
January	46.1269
February	61.8703
March	87.6243
April	121.957
May	174.883
June	220.658
July	259.288
August	250.722
September	209.263

2.7. NDWI (Normalized Difference Water Index)

The NDWI stands as the first-ever proposed index for extracting water information from remote sensing imagery and data. Introduced by McFeeters in 1996, this index utilizes the near-infrared (NIR) and green bands to effectively detect and delineate water bodies. Water exhibits high reflectance in the green band and low reflectance in the near-infrared band. Capitalizing on this distinct spectral behavior, the NDWI is defined using the following formula (McFeeters, 1996):

$$NDWI = \frac{(Green-NIR)}{(Green+NIR)} \quad (1)$$

Leveraging water's distinct spectral characteristic of higher reflectance in the green wavelength compared to the near-infrared wavelength, the NDWI effectively minimizes the influence of non-water features such as soil and vegetation. (McFeeters et al., 1996) proposed a threshold value of zero for NDWI, where positive values indicate the presence of water and negative values represent non-water features like soil and vegetation cover.

The Normalized Difference Water Index (NDWI) is a spectral index used to identify and assess water content within vegetation and water bodies. NDWI values can be positive or negative, each carrying distinct interpretations. Negative NDWI values typically indicate areas with very low or no water content, such as arid soils, bare rocks, urban areas, or other non-water surfaces. Conversely, low NDWI values, particularly those below 0.1, are often indicative of dry soils or regions with extremely low moisture content. In essence, negative NDWI values signify a dearth of water content, while low NDWI values below 0.1 are more specifically associated with arid soils or extremely dry regions. These interpretations are generally based on the spectral behavior of different materials in the green and near-infrared bands.

2.8. Principal component analysis

To examine the primary climate factors affecting rainfall events in the study area, this research employs the Principal Component Analysis (PCA) technique. PCA aims to explain the maximum possible variance observed in a set of variables using the minimum number of components. PCA transforms a set of initially correlated variables into a new set of uncorrelated variables, termed principal components or factors. These principal components are linearly related to the original variables and are ranked based on their percentage of explained total variance. Among these principal components, those that explain the most cumulative variance are selected, leading to a reduction in the overall data set size (Avila-Vera et al., 2020: 12). These principal components are uncorrelated and retain a substantial portion of the original information. Consequently, a reduced model of principal components (PCA) can be reliably employed to detect and identify anomalies in the original system (Penha et al., 2001: 1). Ultimately, PCA aims to minimize the mean square error. All PCA calculations in this study were performed using XLSTAT and MINITAB software.

2.9. Model Validation Using ANOVA

Following the trend analysis of precipitation at the Aji Chai station for the future period, one-way ANOVA (Analysis of Variance) was applied to examine the presence of significant differences in mean precipitation between distinct time periods. It is important to note that ANOVA is not a novel method but a well-established statistical tool designed to test differences in group means. To ensure its applicability, the Levene test for equality of variances was conducted, as the condition for using ANOVA requires homogeneous group variances. Additionally, the comparison of means between two time periods with unknown variances was performed using a two-sample t-test approach, acknowledging that this test has broader applicability when analyzing datasets with unequal variances. ANOVA's purpose in this study was to validate whether differences in mean precipitation between time periods were statistically significant. However, it does not directly validate the accuracy of predictive models. Instead, it aids in assessing variability in the data across groups. This distinction was critical in contextualizing the use of ANOVA within the broader scope of rainfall analysis and ensuring alignment with its intended statistical applications (Javan Bakht Amini & Khatami, 2005: 13).

2.10. Required parameters for agricultural water demand assessment

To comprehensively evaluate agricultural water demand for a specific site, the following parameters are essential:

1. Annual Activity Level: This refers to the total area of cultivated land within the region. It represents the extent of agricultural activities that contribute to water consumption.
2. Per Capita Water Use: This parameter indicates the average annual water usage per hectare of agricultural land. It reflects the water efficiency of agricultural practices in the area.
3. Monthly Distribution of Agricultural Water Consumption: This information provides a detailed breakdown of water usage throughout

the year, accounting for seasonal variations in crop water requirements and irrigation practices.
4. Consumption Coefficient: This coefficient represents the proportion of withdrawn water that is actually consumed, while the remaining portion is converted into wastewater. It accounts for water losses due to evaporation, seepage, and other factors.
5. New Cropping Patterns: The text mentions three new cropping patterns for the region. These patterns likely represent alternative crop combinations or cultivation strategies with varying water requirements.
6. Monthly Water Requirement per Cropping Pattern: Table 7 presumably provides a detailed breakdown of the monthly water requirements for each of the three new cropping patterns. This information is crucial for assessing the water demand associated with each pattern.

Table 7. Monthly Distribution of Agricultural Water Demand under Different Cropping Patterns

Month	Existing cultivation pattern (1000m3)	Cropping Pattern 1 (1000m3)	Cropping Pattern 2 (1000m3)	Cropping Pattern 3 (1000m3)
September	728.5	1316.6	1433.1	1886.1
October	366.3	376.7	497.5	573.6
November	84.6	31.1	48.7	59.1
December	35.8	0	0	0
January	238.1	112.2	124.9	107.6
February	595.5	1222.6	1273.5	1295.1
March	904.3	2683	2760.3	2775.7
April	701.1	3723.6	3853.8	3837.8
May	712.2	1679.6	1921.5	2004.5
June	879.6	1697.9	1838	2604.5
July	996.2	1824.1	1941.8	2758.7
August	995.9	1842.2	1953.6	2727.3
Yearly	7238.1	16509.6	17646.7	20630

2.11. Regional component modeling in WEAP

WEAP is a comprehensive software tool for modeling and analyzing water resources management at various scales, including regional and basin levels. To effectively model regional components in WEAP, a systematic approach is essential, encompassing the identification of key components, their interactions, and the representation of their characteristics within the modeling framework. Key Components for Regional Modeling are:

1. Rivers: Rivers represent the primary flow paths for water within the region, transporting water from upstream sources to downstream users. In WEAP, rivers are modeled as links that connect different nodes in the system.
2. Upstream Water Rights: Upstream water rights define the allocation of water resources from upstream regions or users. These rights can be incorporated into WEAP through the use of priority rules and allocation mechanisms.
3. Dams and Diversions: Dams and diversions play a crucial role in regulating water flow and diverting water for various purposes. WEAP allows for the modeling of dams with reservoir operations, including storage, release, and hydropower generation. Diversions can be modeled to represent water abstraction for irrigation, municipal, or industrial uses.
4. Agricultural Demand Sites: Agricultural demand sites represent the locations where water is consumed for crop production. WEAP enables the modeling of agricultural water

demand based on crop types, irrigation methods, and seasonal water requirements.

5. Environmental Flow Requirements: Environmental flow requirements represent the minimum amount of water needed to maintain the ecological health of rivers and aquatic ecosystems. WEAP allows for the incorporation of environmental flow requirements into the modeling framework, ensuring that water allocations consider both human and environmental needs.

As illustrated in Figure 5, the modeled water demands, including agricultural and environmental needs, are met by the available water resources from reservoirs and rivers. WEAP's optimization capabilities can be employed to determine the optimal allocation of water resources to meet these demands while considering constraints such as reservoir storage capacity, river flow rates, and water quality requirements. Hydrological systems are inherently complex and dynamic, influenced by various factors such as precipitation, evapotranspiration, groundwater interactions, and human activities. Modeling these systems can be challenging due to the need to accurately represent these complex interactions and account for uncertainties in data and parameters.

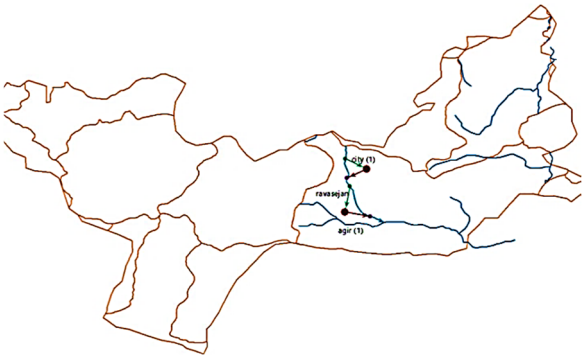

Fig. 5. Schematic Diagram of Regional Component Modeling in WEAP

According to Figure 6, the Kashtanrud River Basin in East Azerbaijan Province, Iran, is formed by two main tributaries.

Northern Tributary: This tributary originates from the southern slopes of Mount Sahand and flows northward.

Southern Tributary: This tributary originates from the northern slopes of Mount Mishu Dagh and flows southward.

Confluence of Tributaries: These two tributaries eventually converge near the city of Tabriz, forming the Kashtanrud River.

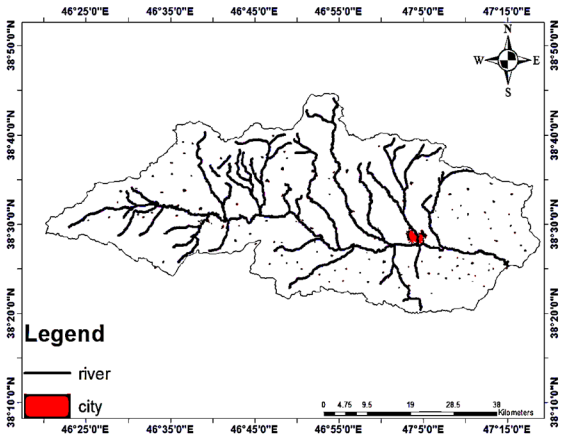

Fig. 6. Stream Modeling in the Study Area

The schematic diagram should clearly indicate that upstream water rights are being diverted from the river. This could be represented by a separate arrow or label indicag the abstraction of water for upstream users. The diagram should also illustrate that the downstream agricultural water rights are met from the reservoir storage. This could be shown by an arrow connecting the reservoir to the downstream irrigation network. The return flow from this irrigation network should be depicted as rejoining the main river at the confluence with Ahar Chai. The diversion weir constructed at Abriq to utilize the flow of the Ravasjan River should be represented in the diagram. This could be shown by a symbol or label at the location of the weir. The existing Abriq irrigation network, covering approximately 1,700 hectares of land, should be clearly marked. However, it should be noted that only 1,200 hectares of this area are currently under irrigated cultivation from the Ravasjan River. The schematic diagram should indicate that a total of 4,800 hectares of land will be covered by the Ithar Dam project. This could be represented by a label or annotation summarizing the total coverage area. The simulation should prioritize water allocation for the existing Ozghan irrigation network, ensuring that their water rights are met under post-dam conditions. This could be represented by a separate label or annotation indicating the priority allocation. The surplus flow regulated and stored in the reservoir should be utilized for the expansion of the Ravasjan irrigation network. This expansion includes:

- Improvement of 500 hectares of existing rainfed lands within the Ravasjan network: This could be shown by a separate label or annotation indicating the improvement of rainfed lands.
- Irrigation of 800 hectares of fallow lands within the network: This could be represented by a separate label or annotation indicating the irrigation of fallow lands.

- Irrigation of 2,300 hectares of land downstream of the Ozghan-Abriq road: This could be shown by a separate label or annotation indicating the irrigation of downstream lands.
- Total expansion area of 3,600 hectares: The total expansion area should be clearly labeled as 3,600 hectares and assigned a priority level of 2 in the simulation.

3. Results and Discussion

3.1. River water level variability

The Fig. 7 illustrates significant fluctuations in the water surface area of the river over the examined period. These fluctuations may stem from various factors, including climate change, intermittent droughts, excessive water extraction for agricultural and industrial purposes, and changes in rainfall patterns. It appears that the river exhibits distinct patterns of high-water and low-water seasons. During certain months of the year, particularly in spring, the water surface area of the river increases significantly, indicating higher rainfall and runoff. Conversely, in summer and autumn, the water surface area decreases sharply, reflecting reduced rainfall and increased evaporation. A general overview of the chart reveals a downward trend in the river's water surface area over time. This decline could indicate a reduction in regional water resources or a rise in water demand. In some years, extreme hydrological events such as floods and prolonged droughts have had a considerable impact on the river's water surface area. These events can lead to sudden and dramatic changes in the river's water volume.

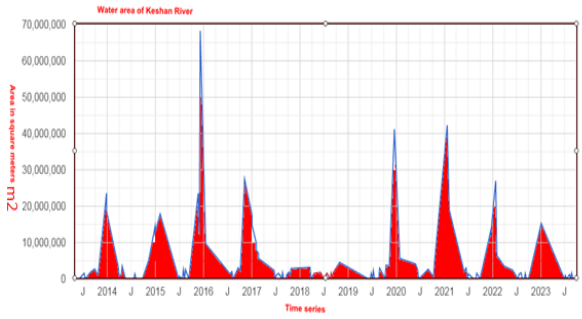

Fig. 7. The time series of the total water surface area of the Kashan River

There are complex interactions among variables such as streamflow, precipitation, evaporation, and temperature. These interactions were addressed in the modeling and analysis through several approaches:

In the WEAP model, interactions are incorporated by:

The relationship between precipitation and surface runoff generation

The interaction between river flow and groundwater levels

The effect of temperature on evapotranspiration

Analysis (PCA) were employed to identify and analyze the relationships and dependencies among variables.

According to Table 8 and Figure 8, the total area of the Kashan River watershed is estimated at approximately 274,937 square kilometers, indicating the vast expanse of this basin. The monthly bars display significant variations in the water surface area of the watershed. Overall, the water surface area is larger during the cold months of the year (winter) compared to the warm months (summer). This highlights the direct impact of rainfall on increasing the water volume in rivers and reservoirs. The largest water surface area is observed in December (568 square kilometers), while the smallest is recorded in November (22 square kilometers), demonstrating a significant difference and emphasizing the sharp fluctuations in the water volume within the watershed. The percentage change column also shows that the monthly variations in water surface area relative to the total watershed area are relatively minor. This is due to the large size of the basin and the minimal impact of local changes on its total area. The Kashan River watershed experiences pronounced seasonal fluctuations in its water levels, primarily influenced by rainfall patterns. Rainfall is the main factor driving changes in the water surface area in this basin, as increased precipitation in winter leads to higher water volumes in rivers and reservoirs. Given the sharp fluctuations in water levels, proper and sustainable management of water resources in this watershed is of great importance.

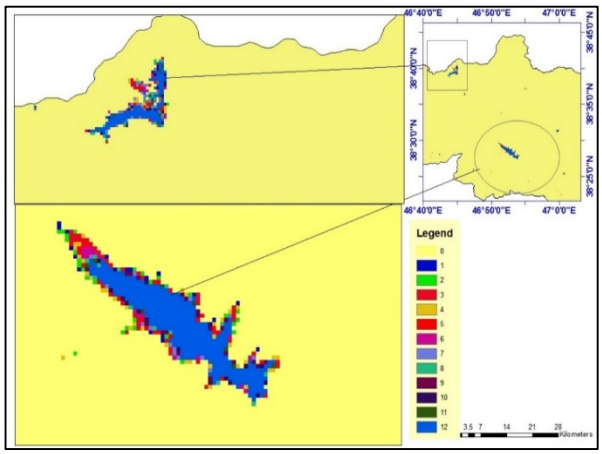

Fig. 8. Temporal and spatial changes in water surface area based on JRC satellite data

Table 8. The area of temporal and spatial water surface changes (square meters) based on JRC satellite data

Code	Monthly	Water Area (in square kilometers)	Percentage
0	No Change	274937	99.599
1	Jan	41	0.015
2	Feb	56	0.020
3	Mar	60	0.022
4	Apr	70	0.025
5	May	54	0.020
6	Jun	49	0.018
7	Jul	44	0.016
8	Aug	50	0.018
9	Sep	53	0.019
10	Oct	41	0.015
11	Nov	22	0.008
12	Dec	568	0.206

Fig. 9 illustrates the changes in the water surface area of the Kashan River watershed over a specified time period. These changes are identified using JRC satellite data with defined temporal and spatial resolution. In this figure, areas with permanent and seasonal surface water are displayed in different colors. Each color in the figure represents a category of water surface area. Dark blue may indicate permanent waters with greater depth, while lighter colors represent seasonal waters or areas with less water coverage.

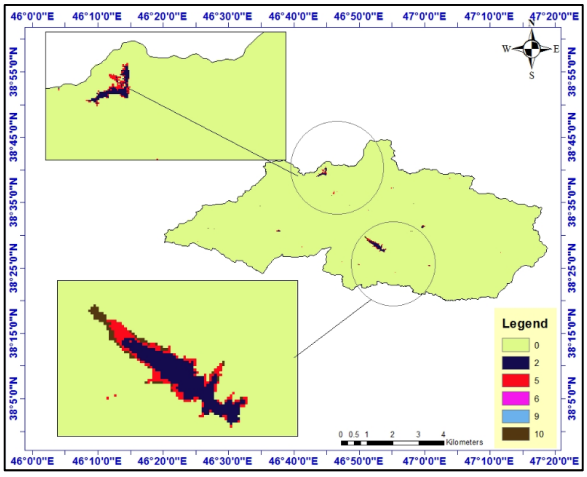

Fig. 9. The trend of the water surface area of the Kashan River using JRC satellite data

Table 9 illustrates the changes in the surface area of different water classes in the Kashan River Lake during the study period. The data are presented as percentages and areas (in square kilometers). The interpretation of these data is as follows:

The unchanged area (code 0) accounts for 99.559% of the lake's surface area (274,828 square kilometers), indicating the stability of the majority of the lake's regions throughout the study period. In other words, most areas of the lake remained constant. The new permanent water area (code 2) constitutes only 0.237% of the lake's surface (653 square kilometers). These areas likely emerged due to changes in water resources or environmental conditions. Additionally, 0.154% of the lake's surface area (426 square kilometers) has been identified as new seasonal water areas (code 5). These regions may only contain water during certain seasons. On the other hand, 0.001% of the surface area (2 square kilometers) is classified as lost seasonal water area (code 6). This change could be attributed to shifts in rainfall patterns or alterations in water resource usage. The transient permanent water area (code 9) also represents 0.001% of the lake's surface (2 square kilometers). These areas may have temporarily appeared as permanent water zones. Finally, 0.049% of the lake's surface area (134 square kilometers) has been identified as transient seasonal water areas (code 10), which likely hold water during specific seasons. Overall, these data indicate that the Kashan River Lake has been relatively stable over the study period, with observed changes primarily limited to permanent and seasonal water areas.

Table 9. Changes in the surface area of different water classes in the Kashan River Lake during the study period

Transition			
Code	Classification	Area (in square kilometers)	Percentage
0	Unchanged Area	274828	99.559
2	New Permanent Water Area	653	0.237
5	New Seasonal Water Area	426	0.154
6	Lost Seasonal Water Area	2	0.001
9	Transient Permanent Area	2	0.001
10	Transient Seasonal Area	134	0.049

3.2. NDWI map and water distribution in Ahar County

The NDWI (Normalized Difference Water Index) map presented in Figure 10 illustrates the spatial distribution of water resources in Ahar County, Iran, from 1990 to 2020. The NDWI is a satellite-based index that effectively differentiates water

bodies from other land cover types, such as soil, vegetation, and rocks.

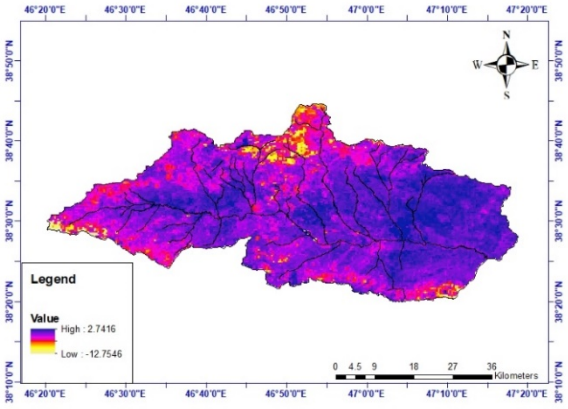

Figure 10. Changes in Water Dynamics in the Keshan chai Basin over 29 Years (1990-2020)

3.3. Water distribution in 1990-1991

During this period, water resources were primarily concentrated in the northern and central parts of Ahar County, exhibiting the highest NDWI values (greater than 0.5). This indicates the presence of high-quality water sources in these regions. In contrast, dry soils dominated the southern and western parts of the county, characterized by the lowest NDWI values (less than 0.1). This reflects water scarcity in these areas (Fig. 11).

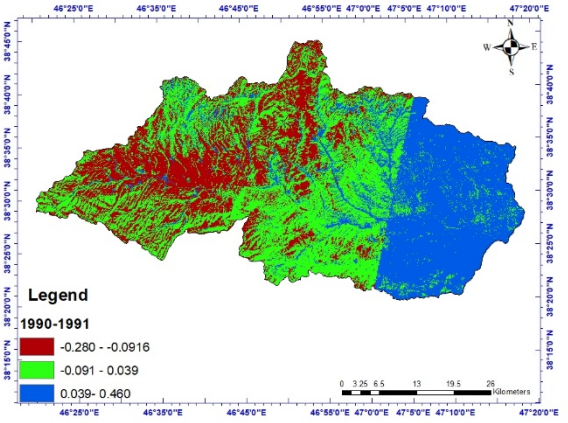

Fig. 11. Spatial distribution of water resources in 1990-1991

3.4. Water Distribution in 2023

Compared to 1990-1991, the spatial distribution of water resources in 2020 reveals noticeable changes. The concentration of water bodies has intensified in the northern and western parts of the county, while it has decreased in some central and southern regions. These changes could be attributed to various factors, including climate variability, human activities, and agricultural expansion (Figure 12).

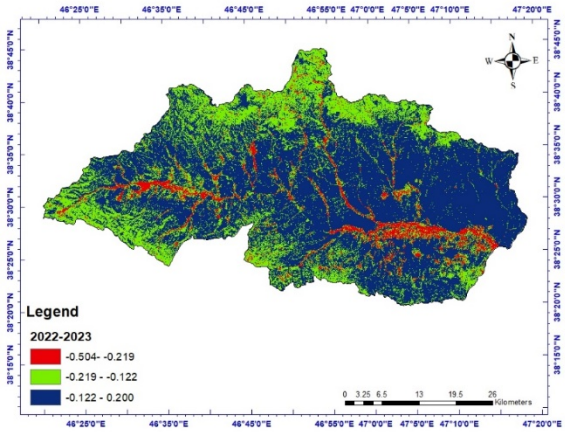

Fig. 12. Spatial distribution of water resources in 2022-2023

The NDWI map presented in this study serves as a valuable tool for understanding the spatiotemporal distribution of water resources in Ahar County. This information can be utilized for effective water resource planning, drought management, and environmental protection strategies. The NDWI difference map presented in the figure illustrates the spatiotemporal changes in water distribution across Ahar County, Iran, over a 30-year period from 1990 to 2023. This map is generated by subtracting the NDWI values in 1990 from the NDWI values in 2023.

Table 10 presents a comparison of the Normalized Difference Water Index (NDWI) for the Keshan chai watershed between the periods 1990-1991 and 2022-2023. The NDWI is employed to assess soil moisture and surface water levels within the region. Color-coded ranges of the NDWI index are utilized to visualize changes in moisture content and water extent over these two periods. In the 2022-2023 period, areas with a severe water deficit (indicated by red) exhibited NDWI values ranging from -0.504 to -0.219, covering an area of 6.25 square kilometers. This signifies a substantial decline in water and moisture content in these regions. Conversely, areas with a milder water deficit (represented by green) had NDWI values between -0.219 and -0.122, encompassing 28.31 square kilometers. These values suggest a less pronounced decrease in moisture compared to the severely affected areas. Additionally, regions with abundant water (dark blue) exhibited NDWI values between -0.122 and 0.200, covering 65.43 square kilometers, indicating a higher presence of water and moisture. In contrast, during the 1990-1991 period, areas with an NDWI between -0.280 and -0.091, spanning 27.15 square kilometers, indicated a severe water deficit. This area was larger than the corresponding area in 2022-2023. Furthermore,

regions with a milder water deficit (green) had NDWI values between -0.091 and 0.039, covering 40.12 square kilometers. Areas with abundant water (dark blue) exhibited NDWI values between 0.039 and 0.460, covering 32.71 square kilometers, which is smaller than the corresponding area in 2022-2023. In conclusion, recent years (2022-2023) have witnessed an increase in areas with abundant water (dark blue), suggesting an improvement in moisture conditions or increased water availability within the Keshan chai watershed. Moreover, the extent of areas with a severe water deficit (red) has decreased compared to the 1990-1991 period, indicating a reduction in water scarcity in recent years. The area of regions with a milder water deficit (green) has also decreased, signifying a relative improvement in water conditions within the region.

Table 10. Comparison of the Normalized Difference Water Index (NDWI) for the Keshan chai watershed between the periods 1990-1991 and 2022-2023.

The humidity of the area	Range of NDWI index	Map color	Area(m2)
Year 2022-2023			
Areas with severe water depletion	-0.504 to -0.219	Red	6.25
Areas with milder water reduction	-0.219 to -0.122	Green	28.31
Areas with high amount of water	-0.122 to 0.2	Dark blue	65.43
Year 1990-1991			
Areas with severe water depletion	-0.28 to -0.091	Red	27.15
Areas with milder water reduction	-0.091 to 0.039	Green	40.12
Areas with high amount of water	0.039 to 0.460	Dark blue	32.71

3.5. Distribution of Water in Ahar County from 1990 to 1991

Fig. 13 presents a comparison of the probability distribution of the Standardized Precipitation Index (SPI) for various time periods. The SPI is an index used to assess drought and wet conditions, with its values indicating the deviation of precipitation from the long-term normal. In this figure, the SPI distribution for the baseline period of 1990-2020 is compared with the SPI distribution in the future period (2025-2065) based on three different climate models. The horizontal axis represents the SPI values, where positive values indicate above-normal precipitation (wet conditions) and negative values indicate below-normal precipitation (drought). The vertical axis represents the probability density of each SPI value, meaning that the higher the curve, the higher the probability of that particular SPI value occurring. Each curve in the graph represents the SPI distribution for a specific time period or climate model. Furthermore, an analysis of the curves corresponding to the future climate models (CNRM-CM6, CanESM5, and CMCC-ESM2) reveals a greater spread compared to the baseline curve (1990-2020). This indicates an increased likelihood of both extremely dry and extremely wet years in the future. Additionally, some models, such as CMCC-ESM2, suggest a potential shift in the mean SPI towards positive values, signifying an overall increase in precipitation. Conversely, models like CNRM-CM6 may indicate a shift towards negative values, suggesting an overall decrease in precipitation. The disparity in the projections provided by different climate models underscores the uncertainty inherent in climate predictions. Based on this figure, it can be anticipated that the precipitation regime of the Keshan chai watershed will undergo significant changes in the future, with an increased likelihood of both extreme drought and wet events. Moreover, the annual average precipitation is projected to either increase or decrease depending on the climate model. These changes may have substantial implications for the lake ecosystem, agriculture, and other water-dependent activities in the region.

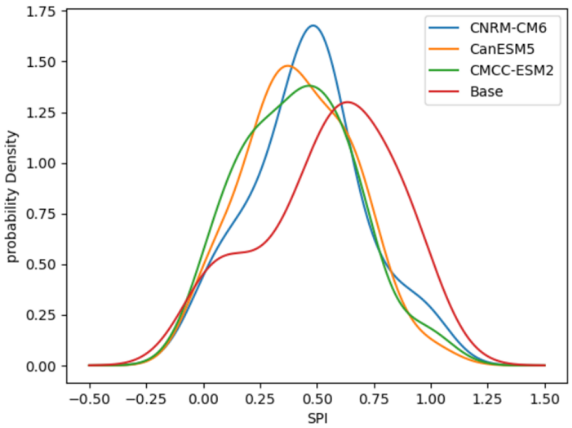

Fig. 13. Probability distribution of Standard Precipitation Index (SPI) for different periods

In Fig. 14, the value of t is 2.045 and the value of p is 0.025. Since the value of p is less than the significance level of 0.05, there is sufficient evidence to reject the null hypothesis. In other words, it can be concluded with 95% confidence that the equality of the average precipitation on the two sides of the figure at the 0.05 significance level

indicates that there will be a trend towards extreme (limit) or a significant decrease in precipitation in the future in the study watershed.

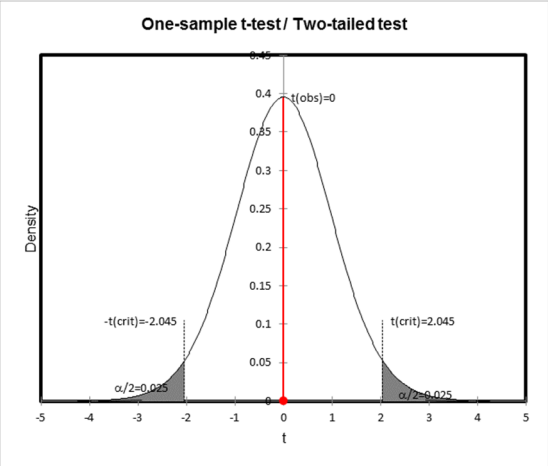

Fig. 14. Probability distribution of precipitation anomalies in the Keshan chai Basin

After entering the data into the MINITAB environment and forming the correlation matrix, the data were analyzed. The precipitation variable was reduced to seven components using the principal component analysis method (with R) and the data were rotated using Varimax rotation. Table (11) shows the percentage of explained variance of the components. The results show that the general factor matrix and the general score matrix are identified, indicating that the monthly precipitation of the watershed in the study area is the result of the interaction of 12 different factors. These factors justify 100% of the total variance with eigenvalues. The highest precipitation in January has provided the highest factor load under severe precipitation conditions, and among the stations studied, January has the highest eigenvalue. The shape diagram test (12) shows the slope or continuous scree plot of the total variance explained by each variable in relation to other variables. As can be seen, the large factors are shown at the top and the other factors are shown with a gradual slope. As can be seen, the first and second components have a steep slope. While the slope of the components becomes gentler from the eighth component onwards and finally turns into a straight line. This study employed a two-sample t-test and a scree plot to provide additional insights into the statistical analysis of the models. The two-sample t-test was utilized to compare the mean values of precipitation between the baseline and future periods under different climate scenarios. This test serves as a complementary analysis to ANOVA by specifically identifying whether the differences between two distinct groups (e.g., baseline vs. future periods) are statistically significant. Unlike ANOVA, which tests differences among multiple groups, the t-test focuses on pairwise comparisons, thereby providing a more detailed understanding of the relationships between specific time periods or models. The scree plot was employed as part of the principal component analysis (PCA) to determine the number of components to retain for subsequent analysis. This graphical tool helps visualize the variance explained by each principal component, enabling researchers to identify the point of inflection (the "elbow") where additional components contribute minimal variance. By focusing on the most significant components, the study effectively reduced dimensionality and highlighted key variables driving changes in precipitation patterns. Additionally, related variables such as precipitation anomalies, temperature changes, and hydrological model outputs were presented in Figure 15. However, to ensure clarity, these variables are now explicitly defined in the text. Precipitation anomalies refer to deviations from the long-term mean precipitation, while temperature changes represent the differences in average temperature between the baseline and future periods. These variables are essential for capturing the impacts of climate change on the hydrological and environmental systems under study. By incorporating both the t-test and scree plot, this research achieves a more nuanced analysis, combining hypothesis testing with dimensionality reduction techniques to comprehensively evaluate climate model performance and projections.

Table 11. Percentage of explained variance of the components

Description	Eigenvalue	Variability (%)	Cumulative %
Jan	2.354	19.616	19.616
Feb	1.917	15.977	35.593
Mar	1.400	11.666	47.259
Apr	1.283	10.692	57.952
May	1.113	9.279	67.231
Jun	1.005	8.376	75.606
Jul	0.851	7.091	82.697
Aug	0.735	6.123	88.819
Sep	0.555	4.629	93.449
Oct	0.329	2.741	96.189
Nov	0.248	2.070	98.259
Dec	0.209	1.741	100.000

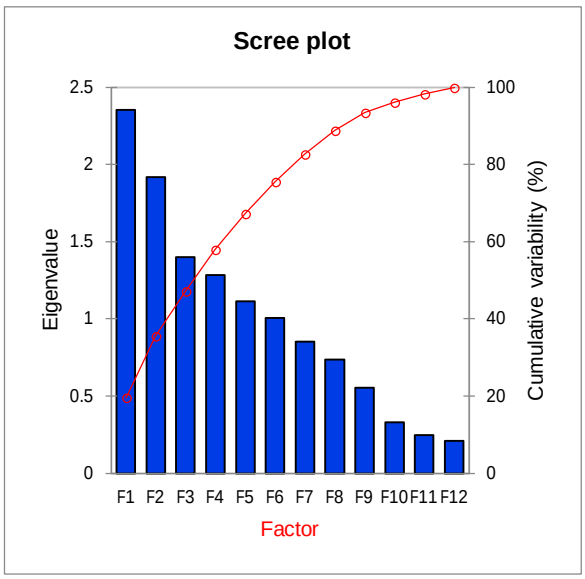

Fig. 15. Scree plot or cumulative variance explained by each principal component

Fig. 16 presents a spatial distribution of monthly precipitation within the study area, allowing for a detailed interpretation. Months positioned closely together exhibit similar precipitation patterns. Conversely, months located further apart demonstrate a negative correlation and significant differences in their precipitation patterns.

Overall, three distinct monthly precipitation patterns are observed in this region:

1. Climate Type 1: This category includes January, February, March, April, June, September, and July. Characterized by high precipitation distribution and density, these months experience heavy rainfall. Their proximity in the 2D plot indicates shared precipitation patterns, likely influenced by dominant seasonal patterns (such as winter or monsoon rains).
2. Climate Type 2: Comprising November, October, and August, this group exhibits moderate precipitation distribution and density. While rainfall intensity is lower compared to Climate Type 1, precipitation is more evenly distributed, potentially associated with transitional seasons.
3. Climate Type 3: December falls under this category, characterized by uniform distribution and low precipitation density. This climate type likely represents a stable precipitation pattern with minimal variations within the month.

The principal components (F1, F2) etc. were extracted from the principal component analysis (PCA) and indicate the directions of maximum changes in the monthly rainfall data in the study area. (first principal component F1) represents 19.62% of the total variance and plays an important role in explaining the general patterns of precipitation changes. It probably represents the main seasonal pattern of precipitation changes and shows the difference in precipitation between months with heavy precipitation and drier months.

(The second principal component F2) represents 15.98% of the variance and is a complement to F1, so that it shows the precipitation changes that F1 could not cover. This component may indicate regional differences or secondary seasonal effects in precipitation patterns.

Considering that F1 and F2 components explain a total of 35.59% of the total variance, these two components can be considered as the main patterns of monthly precipitation changes in catchment area to be used. Subsequent principal components (such as F3, F4, etc.) explain a smaller share of the variance and are likely to indicate more detailed or localized patterns in the data.

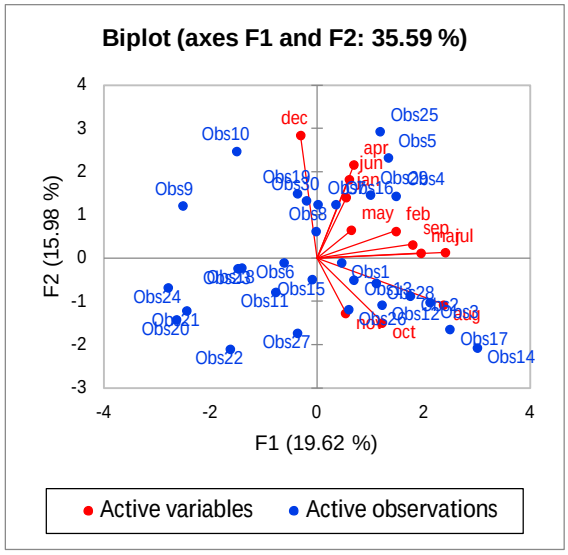

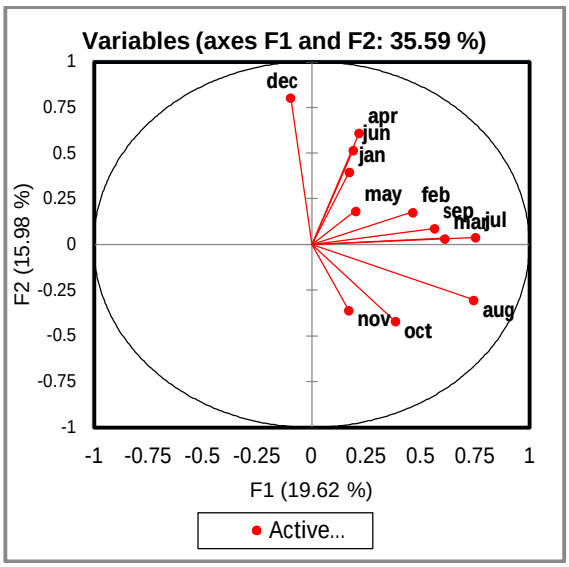

Fig. 16. PCA behavior of monthly precipitation change dispersion in the Karoon River Basin

3.6. Scenario validation

Analysis of Variance (ANOVA), a robust statistical method for comparing means across multiple groups, was employed in this study to identify statistically significant differences in projected precipitation among various climate models. The results of this analysis, presented in Table 12, indicate that the models CMCC-ESM2, CNRM-CM6, and CanESM5 exhibit a significant increase in projected mean precipitation for future periods compared to the baseline scenario. The CNRM-CM6 model estimated a mean precipitation of 614.7 mm with a standard deviation of 107.3 mm, and a 95% confidence interval ranging from 580.9 to 648.4 mm. Similarly, the CMCC-ESM2 model reported a mean precipitation of 504.9 mm with a standard deviation of 137.0 mm and a 95% confidence interval between 471.2 and 538.7 mm. Additionally, for the CanESM5 model, a mean precipitation of 397.3 mm was estimated with a standard deviation of 95.2 mm and a 95% confidence interval ranging from 363.6 to 431.0 mm. Finally, during the observational period (1990-2020), the mean precipitation was recorded as 253.9mm with a standard deviation of 85.4 mm and a 95% confidence interval between 215.1 and 292.7mm. In the "Grouping" column, the letters A, B, C, and D have been assigned to each model to represent groups with significantly different mean precipitation. According to Tukey's method, if two models do not share a common letter, their mean precipitation is significantly different. The CNRM-CM6 model belongs to group A and exhibits the highest mean precipitation, while the CMCC-ESM2 model falls into group B, indicating a lower mean precipitation than CNRM-CM6 but higher than the other models. Furthermore, the CanESM5 model is categorized in group C, exhibiting a significantly lower mean precipitation compared to the CNRM-CM6 and CMCC-ESM2 models. The baseline data (1990-2020) is classified in group D and displays the lowest mean precipitation among all models. Overall, the CNRM-CM6 and CMCC-ESM2 models project a significantly higher mean precipitation for the future period (2025-2065) compared to the baseline. The CanESM5 model also indicates an increase in precipitation relative to the baseline, although the magnitude is significantly lower than the CNRM-CM6 and CMCC-ESM2 models. These results suggest that the baseline data represents the lowest precipitation levels, which are significantly different from the future period, indicating a potential increase in precipitation in the coming years.

Table 12. Grouping Information Using the Tukey Method and 95% Confidence

Factor	Time	N	Mean(mm)	StDev (mm)	Lower bound (95%)	Upper bound (95%)	Grouping			
CNRM-CM6	2025-2065	41	614.7	107.3	580.9	648.4	A			
CMCC-ESM2	2025-2065	41	504.9	137.0	471.2	538.7		B		
CanESM5	2025-2065	41	397.3	95.2	363.6	431.0			C	
Base	1990-2020	31	253.9	85.4	215.1	292.7				D

Analysis of Variance (ANOVA), a robust statistical method for comparing means across multiple groups, was employed in this study to identify statistically significant differences in projected precipitation among various climate models. The results of this analysis, presented in Table 7, indicate that the models CMCC-ESM2, CNRM-CM6, and CanESM5 exhibit a significant increase in projected mean precipitation for future periods compared to the baseline scenario. It is important to note that the earlier reference to RCP scenarios in the text was incorrect, as this study explicitly utilizes SSP scenarios from CMIP6. Specifically, SSP5-8.5 was selected for its representation of a high-emission scenario to evaluate the potential impacts of climate change on precipitation. This correction ensures consistency between the earlier analysis and the results presented in Table 7. Future studies may benefit from exploring additional SSP pathways to provide a broader understanding of the projected impacts. The CNRM-CM6 model estimated a mean precipitation of 614.7 mm with a standard deviation of 107.3 mm and a 95% confidence interval ranging from 580.9 to 648.4 mm. Similarly, the CMCC-ESM2 model reported a mean precipitation of 504.9 mm with a standard deviation of 137.0 mm and a 95% confidence interval between 471.2 and 538.7 mm. Additionally, for the CanESM5 model, a mean precipitation of 397.3 mm was estimated with a standard deviation of 95.2 mm and a 95% confidence interval ranging from 363.6 to 431.0 mm. Finally, during the observational period (1990-2020), the mean precipitation was recorded as 253.9 mm with a standard deviation of 85.4 mm and a 95% confidence interval between 215.1 and 292.7 mm. In the "Grouping" column, the letters A, B, C, and D have been assigned to each model to represent groups with significantly different mean precipitation. According to Tukey's method, if two models do not share a common letter, their mean precipitation is significantly different. The CNRM-CM6 model belongs to group A and exhibits the highest mean precipitation, while the CMCC-ESM2 model falls into group B, indicating a lower mean

precipitation than CNRM-CM6 but higher than the other models. Furthermore, the CanESM5 model is categorized in group C, exhibiting a significantly lower mean precipitation compared to the CNRM-CM6 and CMCC-ESM2 models. The baseline data (1990-2020) is classified in group D and displays the lowest mean precipitation among all models. Overall, the results suggest that the baseline data represents the lowest precipitation levels, which are significantly different from the future period, indicating a potential increase in precipitation in the coming years under the SSP5-8.5 scenario.

Table 13 presents the predicted precipitation values from four different climate models. Each model provides the predicted precipitation amount, standard error, t-statistic, and p-value. The intercept value is 396.266 mm, indicating that, in the absence of other influencing factors, an average of 396.266 mm of precipitation is expected in the Keshan chai basin. The CMCC-ESM2, CNRM-CM6, and CanESM5 models provide varying precipitation predictions compared to the baseline model. The CMCC-ESM2 model predicts a significant increase in precipitation, while the CanESM5 model does not predict any change. The CNRM-CM6 model also forecasts a substantial increase in precipitation, although to a lesser extent than the CMCC-ESM2 model. In other words, if no other variables are considered for precipitation prediction, the expected precipitation in the Keshan chai basin is 283.4 mm. The CMCC-ESM2 model predicts the highest precipitation amount across all years. The extremely low p-values, all less than 0.0001, indicate that the observed differences between the models are statistically significant. In other words, these differences are highly unlikely to be due to chance, and the different models provide distinct precipitation predictions. The baseline model underpredicts the reference precipitation by 143.39 mm. The CMCC-ESM2 model, with a 129.04 mm underprediction compared to the baseline, ranks second in terms of the lowest predicted precipitation. Conversely, the CNRM-CM6 model, with a 218.41 mm overprediction compared to the baseline, predicts the highest precipitation amount.

Table 13. Summary of ANOVA for Baseline and SSP5.85 Scenarios

Source	Value(mm)	Standard error(mm)	T	Pr > |t|	Lower bound (95%)	Upper bound (95%)
Intercept	396.266	16.057	24.679	< 0.0001	364.537	427.995
Base-Base	-143.392	24.702	-5.805	< 0.0001	-192.204	-94.581
Base-CMCC-ESM2	129.038	22.708	5.682	< 0.0001	84.166	173.909
Base-CNRM-CM6	218.412	22.708	9.618	< 0.0001	173.541	263.284
Base-CanESM5	0.000	0.000				

According to Figure (17) and Table (13), it is predicted that annual precipitation in the study area will increase by an average of 5% during the prediction period (2025-2065) compared to the observation period (1990-2020). This increase in precipitation is observed at above 95% confidence level with a value of 427.99 mm and at the lowest level with a value of 364.53 mm. In other words, it will vary between 427.99 and 364.53 in the future period. The CNRM-CM6 and CMCC-ESM2 models have a better fitting performance than the CanESM5 model. Figure (13) shows a boxplot of the changes in precipitation in the future period compared to the observation period. This chart shows the distribution of standardized coefficients for each model. The center line of the box shows the median of the coefficients. To better understand the importance of global warming, it is necessary to examine the annual changes in precipitation. The standard deviation of mean annual precipitation over several years indicates the amount of change in mean precipitation during that time period. However, these changes are not regular in the climate models studied. But ultimately, the Standardized coefficients indicators in the chart show that the CNRM-CM6 model has a better ability to simulate precipitation. The standardized coefficient only shows the intensity of precipitation and does not provide information about the frequency or duration of the study period. On the other hand, the closer the box of the chart is to the y-axis (at the 95% significance level), the more certain the results are in that model.

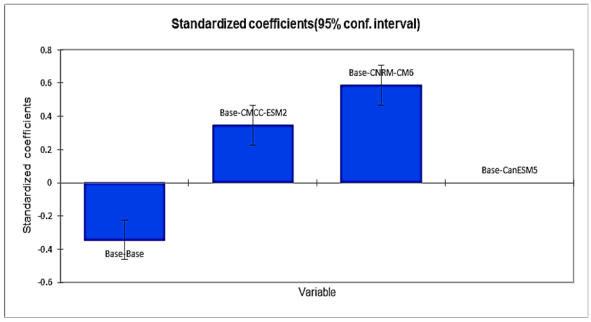

Fig. 17. Distribution of Standardized Coefficients for Selected Models, Future and Observation Periods

In this study, uncertainties related to flow forecasting particularly those arising from differences among various climate models in predicting precipitation (a key driver of streamflow) were evaluated using statistical methods. Specifically, Analysis of Variance (ANOVA) and Tukey's post-hoc test were applied to assess the significance of differences among the precipitation outputs from different climate models. ANOVA, as a robust tool for comparing group means, enabled us to identify statistically significant differences among outputs of the CNRM-CM6, CMCC-ESM2, and CanESM5 models, compared to the baseline data (1990–2020). These results are presented in Table 12 of the manuscript. Tukey's test was then employed to categorize the models into statistically distinct groups (A to D) at a 95% confidence level. For instance, the CNRM-CM6 model, which predicted the highest mean precipitation, fell into group A, while the baseline data were classified in group D, indicating the lowest values. This grouping highlights the range of variability among model outputs and thus the level of uncertainty in precipitation projections. Furthermore, 95% confidence intervals were calculated for each model's precipitation estimate, providing a quantitative measure of uncertainty and a range for possible future changes. These statistical assessments were considered in interpreting the final results and discussing the implications of climate model selection on water resource projections. In summary, the uncertainty stemming from the choice of climate model was explicitly evaluated and incorporated into the results through statistical analysis and interpretation.

The findings of this study can be generalized to other watersheds with similar climatic and hydrological characteristics, such as mountainous basins in northwestern Iran. However, for regions with significantly different conditions (e.g., arid or flat plains), model recalibration and site-specific validation would be necessary. It is important to note that the study is based on real observed data and employs standard and widely accepted modeling tools, which lends a relatively high level of credibility and potential for broader applicability under similar environmental settings.

4. General Conclusion

This study aims to investigate the effects of the construction of the Isar Dam on various parameters of the basin's water resources, including stored water volume, river flow, and water quality, considering climatic conditions. The key innovation in this research lies in its integrated approach to assessing the impacts of both dam construction and climate change on water resources in the basin. While many studies have examined the effects of dams or climate change individually, this research combines these two factors to provide a more comprehensive understanding of their combined influence on water availability, quality, and distribution. The selection of model parameters should be based on the intended application and the specific regional conditions.

The models used in this study particularly the WEAP model along with statistical methods such as Principal Component Analysis (PCA) and Analysis of Variance (ANOVA) are designed not only for academic research but also for practical and managerial applications. These models were calibrated using real and local data, including meteorological, hydrological, physiographic, and operational information, which enhances the accuracy and reliability of the results under real-world conditions. Moreover, the scenarios analyzed in this research (such as changes in cropping patterns and the SSP5-8.5 climate scenario) directly address the challenges that organizations like the East Azerbaijan Regional Water Company face in water resources planning and management. Since WEAP is widely used by water management authorities around the world for integrated water resources planning and allows for scenario analysis, shortage evaluation, and adaptation planning, the findings of this study can effectively support operational decision-making, optimal water allocation, climate change adaptation strategies, and the optimization of agricultural practices.

In this study, key parameters such as precipitation, temperature, evaporation, river discharge, and cropping patterns were given special attention because these factors directly affect water allocation and agricultural water demand. Additionally, physiographic data and reservoir operation information were included to simulate the water resources more accurately. For practical and managerial applications, it is recommended that, in addition to hydrological and climatic parameters, economic variables and water demand data be incorporated with high precision to enhance the usability and reliability of the model results in decision-making processes. This perspective is clearly presented in the manuscript to provide useful guidance for future researchers and water resource managers. The results are as follows:

Key Findings:

- The Ravasjan River has experienced significant fluctuations in water flow due to floods and droughts.
- The environmental flow requirement of the river is a minimum monthly flow of 5.0 cubic meters per second, simulated on an annual basis.

- Water demand satisfaction rates under various scenarios were as follows:

  - ❖ Scenario 1: 92% of Ozghan's water demand and 47% of the development network's demand are met in 70% of cases, while both are fully satisfied in 30% of cases.
  - ❖ Scenario 2: 90% of Ozghan's demand and 45% of the development network's demand are met in 70% of cases, with full satisfaction in 25% of cases.
  - ❖ Scenario 3: 77% of Ozghan's demand and 38% of the development network's demand are met in 70% of cases, while full satisfaction occurs in 23% of cases.

- The dam will provide 14 million cubic meters of regulated water annually for drinking purposes, 35 million cubic meters for agriculture, and 4 million cubic meters for environmental releases.

Climate Change Impacts:

- Simulations indicate a heightened risk of flooding in the study area due to increased precipitation and runoff under climate scenario SSP5.85.
- Precipitation variability between 2011 and 2020 poses challenges for agriculture, water resource management, and other water-sensitive sectors.
- Future precipitation in the watershed is predicted to reach extreme levels, with distinct climatic patterns emerging across different months.
- Principal component analysis reveals that 62.19% of precipitation variance is explained by the first component, while 15.98% is explained by the second.

limitations of this research:

- Focus on a Single Dam: The study primarily focuses on the potential impacts and benefits of the Isar Dam. It may not fully consider the potential impacts of other water infrastructure projects or interventions in the region.
- Limited Scope of Climate Change Scenarios: While the study utilizes the SSP5.85 scenario, it may not fully capture the range of potential climate change impacts. Exploring other scenarios, such as those with more severe or less severe climate change impacts, could provide a more robust assessment.
- Data Limitations: The accuracy of the study's findings may be limited by the availability and quality of historical data, particularly regarding water flow, precipitation, and climate variables.
- Model Limitations: The WEAP model, while a powerful tool, has inherent limitations and assumptions. The accuracy of the model's predictions depends on the quality of input data and the appropriateness of the model's parameters.
- Lack of Socioeconomic Considerations: The study may not fully account for the socioeconomic impacts of the dam, such as potential displacement of communities, changes in land use patterns, and the socio-economic implications of water allocation decisions.
- Uncertainty in Climate Projections: Climate change projections inherently involve uncertainties. The study may not fully account for the potential range of uncertainty in future climate conditions, which could significantly impact the accuracy of the predictions.

References

Agha Karami M, and Moridi A, "Quantitative evaluation of water allocation scenarios using WEAP (case study: Tehran-Karaj Plain)", The 5th Iran Water Resources Management Conference, 2012.

Avila-Vera M, Rangel-Blanco L, Picazzo-Palencia E, "Application of principal component analysis as a technique to obtain a social vulnerability index for the design of public policies in Mexico", Open Journal of Social Sciences, 2020, 8 (9), 130-145. https://doi.org/10.4236/jss.2020.89009

Bañares EN, Mehboob MS, Khan AR, Cacal JC, "Projecting hydrological response to climate change and urbanization using WEAP model: A case study for the main watersheds of Bicol River Basin, Philippines", Journal of Hydrology: Regional Studies, 2024, 54, 101846. https://doi.org/10.1016/j.ejrh.2024.101846

Change C, "Intergovernmental panel on climate change (IPCC)", CC BY, 1995, 4.

Chawanda CJ, Nkwasa A, Thiery W, Van Griensven A, "Combined impacts of climate and land-use change on future water resources in Africa", Hydrology and Earth System Sciences Discussions, 2023, 1-32. https://doi.org/10.5194/hess-28-117-2024

Ciampittiello M, Marchetto A, Boggero A, "Water resources management under climate change: a review", Sustainability, 2024, 16 (9), 3590. https://doi.org/10.3390/su16093590

Dlamini N, Senzanje A, Mabhaudhi T, "Assessing climate change impacts on surface water availability using the WEAP model: A case study of the Buffalo River catchment, South Africa", Journal of Hydrology: Regional Studies, 2023, 46, 101330. https://doi.org/10.1016/j.ejrh.2023.101330

Feng J, "Optimal allocation of regional water resources based on multi-objective dynamic equilibrium strategy", Applied Mathematical Modelling, 2021, 90, 1183-1203.

https://doi.org/10.1016/j.apm.2020.10.027
Fu G, Charles SP, Chiew FH, "A two-parameter climate elasticity of streamflow index to assess climate change effects on annual streamflow", Water Resources Research, 2007, 43 (11). https://doi.org/10.1029/2007WR005890
Garnier J, Cicerelli RE, de Almeida T, Belo JC, Curto J, Ramos APM, Bonnet MP, "Water resources monitoring in a remote region: earth observation-based study of endorheic lakes", Remote Sensing, 16 (15), 2790. https://doi.org/10.3390/rs16152790
Hamlat A, Habibi B, Guidoum A, Sekkoum M, Kadri CB, Guerroudj A, "Water supply and demand balancing and forecasting in a semi-arid region of Algeria using the WEAP model: a case study of El Bayadh province", Sustainable Water Resources Management, 2024, 10 (1), 34. https://doi.org/10.1007/s40899-023-01006-x
Huang D, Liu J, Han G, Huber-Lee A, "Water-energy nexus analysis in an urban water supply system based on a water evaluation and planning model", Journal of Cleaner Production, 2023, 403,136750. https://doi.org/10.1016/j.jclepro.2023.136750
Javankhah Amiri S, Khatami H, "Investigating the relationship between future air quality index parameters in tehran using regression analysis in 1384", Human and Environment, 2005, 10 (1), 15-28.
Jin H, Fang S, Chen C, "Mapping of the spatial scope and water quality of surface water based on the google earth engine cloud platform and landsat time series", Remote Sensing, 2023, 15 (20), 4986. https://doi.org/10.3390/rs15204986
Kang S, Yin J, Gu L, Yang Y, Liu D, Slater L, "Observation-constrained projection of flood risks and socioeconomic exposure in China. Earth's Future", 2023, 11 (7), e2022EF003308. https://doi.org/10.1029/2022EF003308
Khoramabadi F, Fard Moradinia S, "The prediction of precipitation changes in the Aji-Chai watershed using CMIP6 models and the wavelet neural network", Journal of Water and Climate Change, 2024, jwc2024607. https://doi.org/10.2166/wcc.2024.607
Khoramabadi F, Fard Moradinia S, "The prediction of precipitation changes in the Aji-Chai watershed using CMIP6 models and the wavelet neural network", Journal of Water and Climate Change, 2024, 15 (5), 2141. https://doi.org/10.2166/wcc.2024.607
Li X, Zhao Y, Shi C, Sha J, Wang ZL, Wang Y, "Application of water evaluation and planning (WEAP) model for water resources management strategy estimation in coastal Binhai New Area, China. Ocean and Coastal Management, 2015, 106, 97-109. https://doi.org/10.1016/j.ocecoaman.2015.01.016
Li X, Zhao Y, Shi C, Sha J, Wang ZL, Wang Y, "Application of water evaluation and planning (WEAP) model for water resources management strategy estimation in coastal Binhai New Area, China", Ocean & Coastal Management, 2015, 106, 97-109. https://doi.org/10.1016/j.ocecoaman.2015.01.016
Lovato T, Peano D, Butenschön M, Materia S, Iovino D, Scoccimarro E, Navarra A, "CMIP6 simulations with the CMCC Earth system model (CMCC-ESM2)", Journal of Advances in Modeling Earth Systems, 2022, 14 (3), e2021MS002814. https://doi.org/10.1029/2021MS002814
Malmir M, Mohammadrezapour O, Sharif Azari S, "Evaluation of Climate Change Impacts on Agricultural Water Allocation in Qara Su Watershed, Using WEAP", Journal of Irrigation and Water Engineering, 2016, 6 (23), 143-155.
Martinsen G, Liu S, Mo X, Bauer-Gottwein P, "Joint optimization of water allocation and water quality management in Haihe River basin", Science of the Total Environment, 2019, 654, 72-84. https://doi.org/10.1016/j.scitotenv.2018.11.036
Mcfeeters SK, "The use of the Normalized Difference Water Index (NDWI) in the delineation of open water features", International Journal of Remote Sensing, 1996, 17 (7), 1425-1432. https://doi.org/10.1080/01431169608948714
Mejía SXN, Paz SM, Tabari H, Willems P, "Climate change impacts on hydrometeorological and river hydrological extremes in Quito", Ecuador", Journal of Hydrology: Regional Studies, 2023, 49, 101522. https://doi.org/10.1016/j.ejrh.2023.101522
Moradian S, Taleai M, Javadi G, "A decision support system for water allocation in water scarce basins", Iranian Journal of Remote Sensing & GIS, 2019, 11 (1), 19-32.
Oki T, Sud YC, "Design of total runoff integrating pathways (TRIP) A global river channel network", Earth Interactions, 1998, 2 (1), 1-37. https://doi.org/org/10.1175/1087-3562(1998)002<0001:DOTRIP>2.3.CO;2
Peng T, Zhao L, Wang P, "Water resource safety assessment and limiting factor diagnosis based on improved concept and matter–element analysis models: a case study of a typical karst area in southwest China", Frontiers in Environmental Science, 2024, 12, 1451365. https://doi.org/10.3389/fenvs.2024.1451365
RaziSadath PV, Rinisha Kartheeshwari M, Elango L, "WEAP model-based evaluation of future scenarios and strategies for sustainable water management in the Chennai Basin, India", AQUA-Water Infrastructure, Ecosystems and Society, 2023, 72 (11), 2062-2080. https://doi.org/102166/aqua.2023.1444
Sabbaghi MA, Nazari M, Araghinejad S, Soufizadeh S, "Economic impacts of climate change on water resources and agriculture in Zayandehroud river basin in Iran", Agricultural Water Management, 2020, 241, 106323. https://doi.org/10.1016/j.agwat.2020.106323
SEI, WEAP water evaluation and planning system: user guide for WEAP21. Stockholm Environment Institute, Boston, 2011. https://doi.org/10.5004/dwt.2018.22332
Snizhko S, Didovets I, Shevchenko O, Yatsiuk M, Hattermann FF, Bronstert A, "Southern Bug River: water security and climate changes perspectives for post-war city of Mykolaiv, Ukraine", Frontiers in Water, 2024, 6, 1447378. https://doi.org/10.3389/frwa.2024.1447378
Swart NC, Cole JN, Kharin VV, Lazare M, Scinocca JF, Gillett NP, Anstey J, Arora V, Christian JR, Hanna S, Jiao Y, Lee WG, Majaess F, Saenko OA, Seiler C, Seinen C, Shao A, Sigmond M, Solheim L, Von Salzen K, Yang D, Winter B, "The canadian earth system model version 5 (CanESM5. 0.3). Geoscientific Model Development, 2019, 12 (11), 4823-4873. https://doi.org/10.5194/gmd-12-4823-2019
Technical Studies of Isar Ahar Dam, Faraz Ab Consulting Engineers Company, East Azarbaijan Province, Tabriz, Iran.

Technical Studies of Isar Dam, Faraz Ab Consulting Engineers Company, East Azarbaijan Province, Tabriz, Iran.

Teweldebrihan MD, Dinka MO, "The impact of climate change on the development of water resources", Global Journal of Environmental Science and Management, 2024, 10 (3), 1359-1370. https://doi.org/10.22034/gjesm.2024.03.25

Valcke S, Guilyardi E, Larsson C, PRISM and ENES: A European approach to Earth system modelling. Concurrency and Computation: Practice and Experience, 2006, 18 (2), 247-262. https://doi.org/10.1002/CPE.V18:2

Voldoire A, Saint-Martin D, Sénési S, Decharme B, Alias A, Chevallier M, Waldman R, "Evaluation of CMIP6 deck experiments with CNRM-CM6-1", Journal of Advances in Modeling Earth Systems, 2019, 11 (7), 2177-2213. https://doi.org/10.1029/2019MS001683

Wang K, Davies EG, Liu J, "Integrated water resources management and modeling: A case study of Bow River basin, Canada", Journal of Cleaner Production, 2019, 240, 118242. https://doi.org/10.1016/j.jclepro.2019.118242

Yaghoubi B, Hosseini SA, Nazif S, Daghighi A, "Development of reservoir's optimum operation rules considering water quality issues and climatic change data analysis", Sustainable Cities and Society, 2020, 63, 102467. https://doi.org/10.1016/j.scs.2020.102467

Zhou S, Wang Y, Su H, Chang J, Huang Q, Li Z, "Dynamic quantitative assessment of multiple uncertainty sources in future hydropower generation prediction of cascade reservoirs with hydrological variations", Energy, 2024, 299,131447. https://doi.org/10.1016/j.energy.2024.131447